

Fluorene-containing polyhedral oligomeric silsesquioxanes modified hyperbranched polymer for white light-emitting diodes with ultra-high color rendering index of 96

Mixue Wang^a, Xiaozhen Wei^a, Weixuan Zhang^a, Haocheng Zhao^{b,c}, Yuling Wu^{a,*}, Yanqin Miao^a, Hua Wang^{a,**}, Bingshe Xu^a

^a Key Laboratory of Interface Science and Engineering in Advanced Materials, Taiyuan University of Technology, Taiyuan 030024, China

^b Department of Electrical Engineering, Shanxi Institute of Energy, Taiyuan 030600, China

^c College of Materials Science and Engineering, Taiyuan University of Science and Technology, Taiyuan 030024, China

ARTICLE INFO

Keywords:

Polymer light-emitting diodes

White light

Color rendering index

Polyhedral oligomeric silsesquioxanes

Hydrophobicity

ABSTRACT

In this work, a series of hyperbranched white-emitting conjugated polymers were synthesized with polyfluorene (PF) as the branches and three-dimensional-structured spiro[3.3]heptane-2,6-dispirofluorene (SDF) as the conjugated branching point by one-pot Suzuki polycondensation, where 4,7-dithienyl-2,1,3-benzothiadiazole (DBT) as orange-light emitting unit and fluorene-containing polyhedral oligomeric silsesquioxanes (POSSs) as conjugated linking monomer were introduced into the backbones to obtain white-light emission. The influence mechanism of POSSs for hyperbranched white-emitting polymers was explored by adjusting the feeding ratios of fluorene-containing POSSs (from 1 to 20 mol%). The results indicated that the synthesized polymers still maintained the high thermal stabilities, and exhibited the improved amorphous film morphology and hydrophobicity, which were beneficial for obtaining optimized interface between the aqueous hole transport layer Poly(3,4-ethylenedioxythiophene)-poly(styrenesulfonate) (PEDOT: PSS) layer and polymer light-emitting layer in device fabrication. As a consequence, all of the fabricated devices with the hyperbranched polymers as light-emitting layers realized white light-emission, and the optimized device exhibited good electroluminescent (EL) performance with Commission Internationale de l'Eclairage (CIE) coordinates at (0.32, 0.33) and maximum color rendering index (CRI) of 96. The fluorene-containing POSSs modified hyperbranched copolymers with broad full width at half maximum (>284 nm) are attractive candidates for sunlight-style white polymer light-emitting diodes.

1. Introduction

White polymer light-emitting diodes (WPLEDs) have been widely recognized towards their potential applications in large area full-color and flexible displays combined with a color filter, backlights and solid lighting sources because they are low-carbon and environmentally friendly planar light source [1–6] to produce highly efficient saturated white-light with high luminance and low driving voltage [7–9]. In particular, compared with linear polymers, the three-dimensional structured hyperbranched polymers can increase steric hindrance, effectively avoid the fluorescence quenching and crystallization caused by the π - π stacking of the molecules, thereby improving the light-emitting

performance of the polymers and the electroluminescence of the corresponding devices [10–15].

In our previous research, in order to improve the luminance, efficiency, and stability of the hyperbranched polymer light-emitting diodes (PLEDs), phosphorescent red emitter of bis(1-phenylisoquinoline)(acetylacetonato)iridium(III) (Ir(piq)₂acac) with high luminescent quantum yield and fluorescent blue emitter of carbazole with excellent thermal stability had been introduced to hyperbranched white light-emitting polymers. It was found that the introduction of the above groups improved the luminance and efficiency of polymer devices to some extent, but there were still some problems in the stability and lifetime of the devices. This is because part of the PEDOT: PSS layer could

* Corresponding author.

** Corresponding author.

E-mail addresses: wuyuling@tyut.edu.cn (Y. Wu), wanghua001@tyut.edu.cn (H. Wang).

<https://doi.org/10.1016/j.jssc.2021.122122>

Received 24 January 2021; Received in revised form 1 March 2021; Accepted 6 March 2021

Available online 11 March 2021

0022-4596/© 2021 Elsevier Inc. All rights reserved.

be dissolved in the hyperbranched polymer light-emitting layer to form an uneven interface with defects in the spin-coating process when the single light-emitting layer WPLEDs were prepared. As the current density was continuously increased, the defect area was easily broken-down and a lot of heat was generated at the same time, which greatly limited the efficiency and luminance and reduced the stability and lifetime of the device. It is considered molecular modification would be a promising strategy to improve thermostability, antioxidative stability, solubility and hydrophobicity of hyperbranched white light copolymer by introducing functional groups with hydrophobic properties into the side chains of hyperbranched polymers.

Polyhedral oligomeric silsesquioxanes (POSSs) have got considerable interests in the organic light-emitting diode (OLED) field due to their excellent thermal stability, oxidation resistance, mechanical toughness, light transmittance, conductivity, solubility and low surface energy [16–21]. They are considered as multifunctional groups with excellent performance because they can combine the advantages of inorganic materials with those of organic polymers [22,23]. Meanwhile, it is possible to introduce some special groups into POSSs to modify target materials [24–27]. Therefore, the POSSs groups were selected as the best polymer modifiers in this work.

In this work, the hyperbranched white-emitting polymers with 2,7-fluorene branches, spiro[3.3] heptane-2,6-dispirofluorene (SDF) core (10 mol%), and POSSs modified 2,7-fluorene and DBT as light-dimming units were constructed. POSSs were introduced into the polymers as dopant side-chains. The influences of POSSs on their thermal, hydrophobicity, photoluminescent (PL) and EL properties were investigated in detail. It was demonstrated the three-dimensional-structured SDF exhibited excellent morphological stability and intense fluorescence [28], and the POSSs group showed significant improvements in film-forming ability and hydrophobicity. As a consequence, the fabricated devices with synthesized hyperbranched polymers as emission layers (EMLs) realized good white emission with Commission Internationale de l'Eclairage (CIE) at (0.32, 0.33) and maximum color rendering index (CRI) of 96.

2. Experimental section

2.1. Materials and characterization

Dihydropyran, 2-bromoethanol, *p*-toluenesulfonic acid monohydrate, 2,7-dibromofluorene, tetrabutylammonium chloride hydrate, allyl bromide, 5-bromo-1-pentene, 7-bromo-1-heptene, 3,3,3-trifluoropropyltrimethoxysilane, (3-bromopropyl)trichlorosilane, 2,7-dibromo-9,9-dioctylfluorene (**M1**, 99.8%), 9,9-dioctylfluorene-2,7-bis (boronic acid pinacol ester) (**M2**, 99.5%), Aliquant336, tetrakis(triphenylphosphine) palladium, phenylboronic acid, and bromobenzene were purchased from Energy Chemical company and Synwitech company. Tetrahydrofuran (THF) and toluene were distilled using standard procedures. Other solvents were used without further purification unless otherwise specified. All reactions were carried out using Schlenk techniques under a dry nitrogen atmosphere.

¹H NMR spectra were measured on a Bruker DRX 600 spectrometer, and chemical shifts were reported in ppm using tetramethyl silane as an internal standard and using deuterated chloroform (CDCl₃), deuterated acetone (acetone-*d*₆) or deuterated dimethyl sulfoxide (DMSO-*d*₆) as solvents. Molecular weights and polydispersities of the copolymers were determined using gel permeation chromatography (GPC) on an HP1100 HPLC system equipped with a 410 differential refractometer, and a refractive index (RI) detector, with polystyrenes as the standard and THF as the eluent at a flow rate of 1.0 mL/min at 30 °C. Infrared spectra (IR) were measured on a Bruker Tensor 27 infrared spectrometer with KBr crystal as the carrier. Atomic force microscopy (AFM) measurements were performed on a SPA-300HV from Digital Instruments Inc. Thermogravimetric analysis (TGA) of the copolymers was conducted on a Netzsch TG 209 F3 thermogravimetric analyzer at a heating rate of 10

°C/min under nitrogen atmosphere. Differential scanning calorimetry (DSC) measurements were performed at both heating and cooling rates of 5 °C/min under nitrogen atmosphere, using DSC Q100 V9.4 apparatus. The UV–visible absorption spectra were determined on a Hitachi U-3900 spectrophotometer and the PL spectra were obtained using a Horiba FluoroMax-4 spectrophotometer at room temperature. Fluorescence lifetime and fluorescence quantum yield of copolymers were measured on an Edinburgh Instrument FLS980 spectrometer. Cyclic Voltammetry of copolymers were measured on an electrochemical workstation of Shanghai Chenhua Instrument Co. Ltd.

2.2. Syntheses

Spiro[3.3] heptane-2,6-di-(2',2'',7',7''-tetrabromospirofluorene) (TBrSDF) [29–31] and 4,7-bis(2-bromo-5-thienyl)-2,1,3-benzothiazole (DBrDBT) [32–34] were synthesized according to the published literature. The synthesis of the precursor with POSSs **6** is shown in Scheme 1, and the detailed descriptions about ¹H NMR and ¹³C NMR of the precursors (**2–6**) are displayed in Figure S1–S7 in supplementary information.

General Procedure for the Synthesis of copolymers PFSDf10-POSS1, PFSDf10-POSS5, PFSDf10-POSS10, PFSDf10-POSS20.

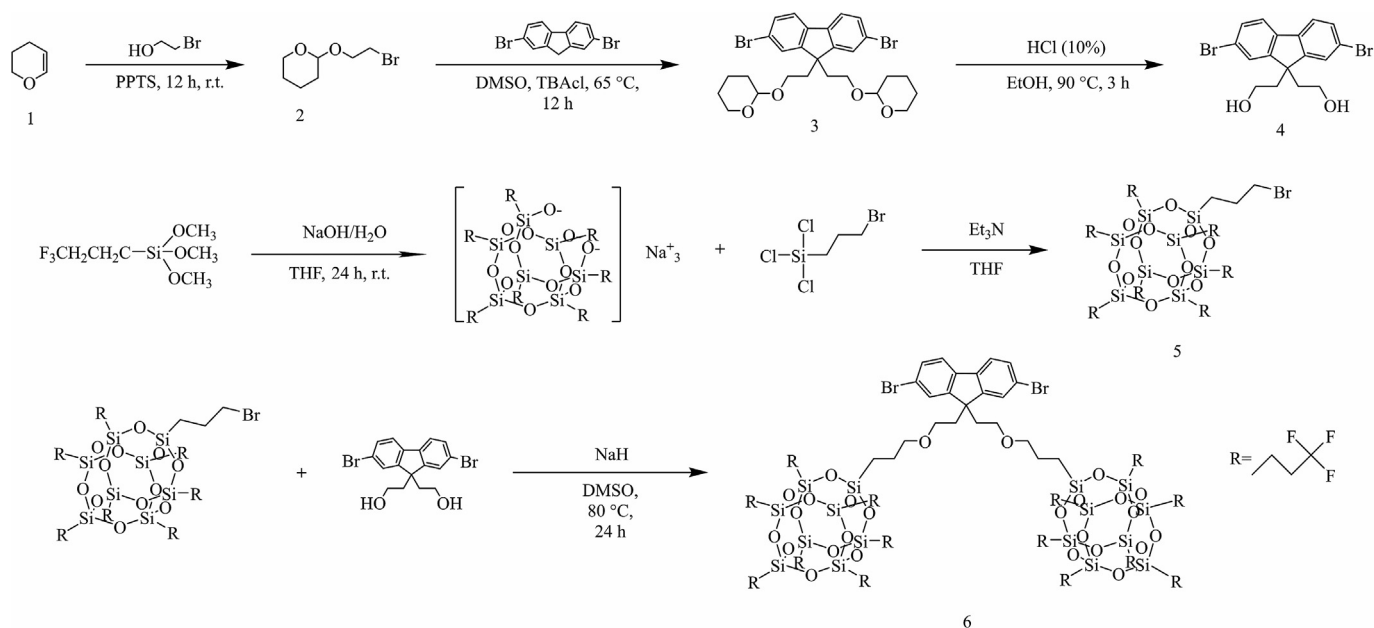
To a solution of predetermined amount of monomers (**M1**, **M2**, POSSs and TBrSDF) in toluene (30 mL) was added an aqueous solution (15 mL) of K₂CO₃ (2 M), a catalytic amount of Pd(PPh₃)₄ (0.10 g, 0.10 mmol) under nitrogen. Aliquat 336 (2 mL) in toluene (5 mL) was added as the phase transfer catalyst. The mixture was vigorously stirred at 100 °C for 72 h. Then DBrDBT (3.20 mL, 2 × 10⁻³ mol/L) was added and the mixture was continuously stirred at 100 °C for 48 h. Phenylboronic acid (0.14 g, 1.00 mmol) in toluene (10 mL) was then added to the reaction mixture, followed by stirring at 100 °C for an additional 12 h. Finally, bromobenzene (2 mL) was added by heating for 12 h again. When cooling to room temperature, the reaction mixture was washed with 2 M HCl and water. The organic layer was separated, and the solution was added dropwise to excess methanol. The precipitated polymers were collected by filtration and dried under vacuum. The solid was Soxhlet extracted with acetone for 48 h and then passed through a short chromatographic column using toluene as the eluent to afford the polymers. The detailed descriptions about ¹H NMR of the copolymers are displayed in Figure S8 in supplementary information.

PFSDf10-POSS1 : **M1** (0.37 g, 0.68 mmol), **M2** (0.71 g, 1.10 mmol), TBrSDF (0.14 g, 0.20 mmol), POSSs (0.06 g, 0.02 mmol) and DBrDBT (3.20 mL, 2 × 10⁻³ mol/L). Gray powder, yield: 48.5%. ¹H NMR (600 MHz, CDCl₃) δ(ppm) : 8.08–7.40 (-ArH-), 7.01–6.75 (-ArH-), 3.44–2.92 (-CH₂-), 2.66–2.53 (-CH₂-), 2.20–1.78 (-C-CH₂-), 1.24–1.09 (-CH₂-), 1.09–0.94 (-CH₃-), 0.94–0.58 (-CH₂-).

PFSDf10-POSS5 : **M1** (0.33 g, 0.60 mmol), **M2** (0.71 g, 1.10 mmol), TBrSDF (0.14 g, 0.20 mmol), POSSs (0.27 g, 0.10 mmol) and DBrDBT (3.20 mL, 2 × 10⁻³ mol/L). Deep gray powder, yield: 52.6%. ¹H NMR (600 MHz, CDCl₃) δ(ppm) : 7.86–7.29 (-ArH-), 6.93–6.70 (-ArH-), 3.43–2.91 (-CH₂-), 2.58–2.31 (-CH₂-), 2.16–1.78 (-C-CH₂-), 1.24–1.18 (-CH₂-), 1.18–0.92 (-CH₃-), 0.92–0.58 (-CH₂-).

PFSDf10-POSS10 : **M1** (0.27 g, 0.50 mmol), **M2** (0.71 g, 1.10 mmol), TBrSDF (0.14 g, 0.20 mmol), POSSs (0.54 g, 0.20 mmol) and DBrDBT (3.20 mL, 2 × 10⁻³ mol/L). Deep gray powder, yield: 46.2%. ¹H NMR (600 MHz, CDCl₃) δ(ppm) : 8.03–7.31 (-ArH-), 6.93–6.80 (-ArH-), 3.45–2.72 (-CH₂-), 2.61–2.31 (-CH₂-), 2.18–1.77 (-C-CH₂-), 1.24–1.18 (-CH₂-), 1.18–0.92 (-CH₃-), 0.92–0.50 (-CH₂-).

PFSDf10-POSS20 : **M1** (0.16 g, 0.30 mmol), **M2** (0.71 g, 1.10 mmol), TBrSDF (0.14 g, 0.20 mmol), POSSs (1.07 g, 0.40 mmol) and DBrDBT (3.20 mL, 2 × 10⁻³ mol/L). Deep gray powder, yield: 45.3%. ¹H NMR (600 MHz, CDCl₃) δ(ppm) : 8.01–7.42 (-ArH-), 6.94–6.75 (-ArH-), 3.39–2.99 (-CH₂-), 2.60–2.35 (-CH₂-), 2.18–1.78 (-C-CH₂-), 1.23–1.17 (-CH₂-), 1.17–0.94 (-CH₃-), 0.85–0.62 (-CH₂-).



Scheme 1. Synthetic route of precursor 6.

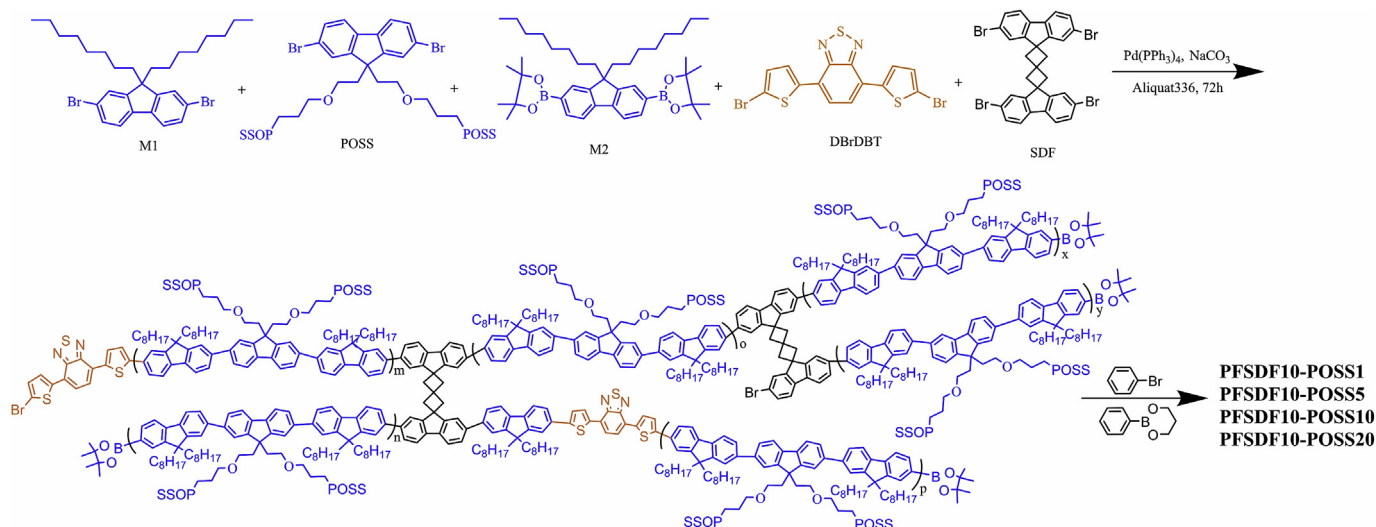
3. Results and discussion

3.1. Synthesis and characterization

The fluorene-containing polyhedral oligomeric silsesquioxanes (POSSs) monomer **6** (Scheme 1) and modified hyperbranched copolymers PFSDf10-POSSx with 9,9-dioctylfluorene and **6** as the branches, SDF as the branching point and DBT as light-dimming units were prepared by Suzuki polycondensation (Scheme 2). According to previous research work [35], the proportion of branching point SDF was selected at 10 mol%. At the same time, in order to obtain white light emission, the organic light-emitting unit DBT was incorporated into the backbone at a feed ratio of 6.4×10^{-6} mol with respect to the blue light-emitting groups of all copolymers. After that, we adjusted the feed ratio of the POSSs modified 9,9-dioctylfluorene so as to get the best synergy between the cage structure and branching point SDF, named as PFSDf10-POSS1 (1 mol%), PFSDf10-POSS5 (5 mol%), PFSDf10-POSS10 (10 mol%) and PFSDf10-POSS20 (20 mol%), respectively. The yields of the copolymer varied from 45% to 53%. Table 1 summarizes the

synthesis and structure parameters of all copolymers.

As shown in Fig. 1a, we verified the structure of the monomers and polymers by infrared spectroscopy, where $600\text{--}500\text{ cm}^{-1}$ is the stretching vibration peak of the C–Br bond in TBrSDF and **M1**. At the same time, 1352 cm^{-1} is the stretching vibration peak of the B–O bond in **M2**. The above-mentioned vibration peaks disappeared in the copolymer PFSDf10-POSS1, indicating that the copolymer was successfully obtained. As shown in Fig. 1b, the antisymmetric stretching vibration peak at $2924\text{--}2850\text{ cm}^{-1}$ and 2912 cm^{-1} are the C–H bands of polyfluorene alkyl chain and the spiro C–H bands of TBrSDF, which shows that SDF has been successfully incorporated into the copolymers. The peak at $1650\text{--}1430\text{ cm}^{-1}$ is the C=C stretching vibration peak of benzene ring skeleton. Obviously, the peaks at 1132 cm^{-1} and 1234 cm^{-1} are the stretching vibration peaks of the C–O bond and C–Si bond connecting between POSSs and fluorene. Then the characteristic bands of POSSs at $1145\text{--}1074\text{ cm}^{-1}$ can be assignable to the stretching vibration of Si–O–Si bonds, which were clearly exhibited in the FTIR spectrum and Si–O–Si stretching bands became more intensified with increasing the POSSs ratio. Simultaneously, a strong C–F stretching band at $1300\text{--}1120$



Scheme 2. Synthetic route of the copolymers.

Table 1
Polymerization results and characterization of the copolymers.

Copolymers	n_{M1} (mol)	n_{M2} (mol)	n_{TBrSDF} (mol)	n_{DBrDBT} (mol)	n_{POSS} (mol)	yield (%)	GPC		
							M_n	M_w	PDI
PFSDf10-POSS1	0.68	1.10	0.20	6.4×10^{-6}	0.02	48.5	11,112	38,517	3.46
PFSDf10-POSS5	0.60	1.10	0.20	6.4×10^{-6}	0.10	52.6	8381	16,500	1.97
PFSDf10-POSS10	0.50	1.10	0.20	6.4×10^{-6}	0.20	46.2	7250	14,495	2.00
PFSDf10-POSS20	0.30	1.10	0.20	6.4×10^{-6}	0.40	45.3	6543	13,992	2.13

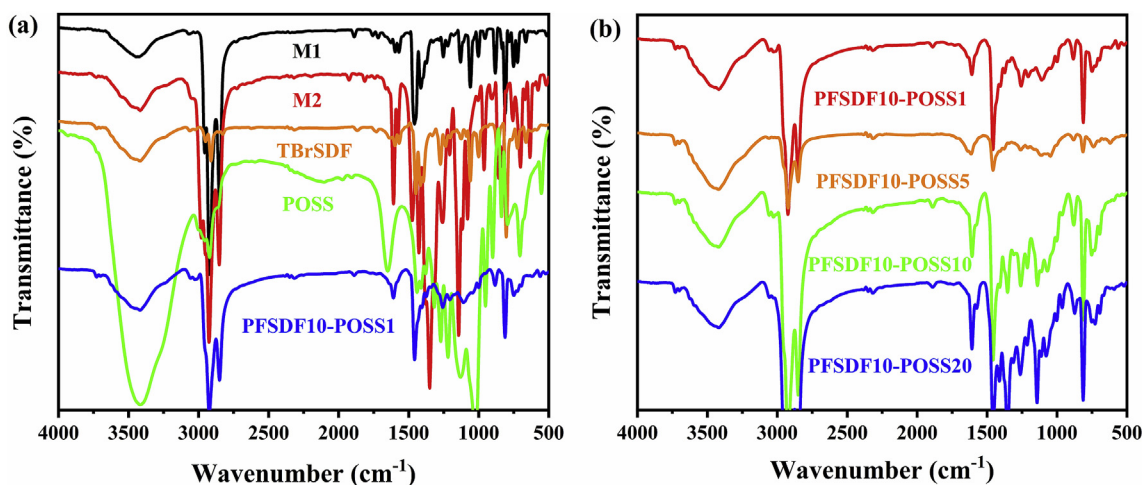


Fig. 1. (a) FT-IR spectra of monomers and copolymers (M1:2,7-Dibromo-9,9-dioctylfluorene, M2:9,9-Dioctylfluorene-2,7-bis (boronic acid pinacol ester), TBrSDF, POSSs, P1:PFSDf10-POSS1), (b) FT-IR spectra of copolymers.

cm^{-1} was observed from FT-IR [19]. This proved that the POSSs were successfully attached to the polymer chain.

In addition, the structure of the polymers was verified by ^1H NMR. As can be seen from Figure S8, the peak integral intensities of the proton signals around the ether bond on the side chain (δ 3.45–3.00) compared with the alkyl chain of fluorene (δ 1.24–1.09) of the polymers was gradually enhanced from PFSDf10-POSS1 to PFSDf10-POSS20, which was consistent with the increasing trend of POSSs content.

The GPC characterization results are shown in Table 1. The number-average molecular weights (M_n) of the copolymers were determined ranging from 6543 to 11,112 with a polydispersity index (PDI) from 1.97 to 3.46. The copolymers were readily soluble in common organic solvents, such as chloroform, tetrahydrofuran, toluene, etc. The insufficient molecular weight of PFSDf10-POSS10 and PFSDf10-POSS20 may be attributed to the fact that the POSSs groups introduced on the 9th carbon atom of fluorene by alkyl chains provided steric hindrance in the

synthesis of the polymers, leading to a decreased molecular weight of the polymers.

3.2. DFT calculation

As shown in Fig. 2, the density functional theory (DFT) calculation was performed on POSSs monomer, and the B3LYP/6-31G(d) method was used to optimize the molecule configuration. The size of the Si–O–Si skeleton of POSSs molecule with a cage-like three-dimensional structure is 0.42 nm. At the same time, the size of POSSs monomer after the introduction of the divergent trifluoropropyl group was significantly increased to 0.92 nm due to the accumulation of molecular chains. The highest occupied molecular orbital (HOMO) of monomer is mostly localized on the alkyl chain attached to the fluorene, while the lowest unoccupied molecular orbital (LUMO) is mainly localized on the cage structure and its interior.

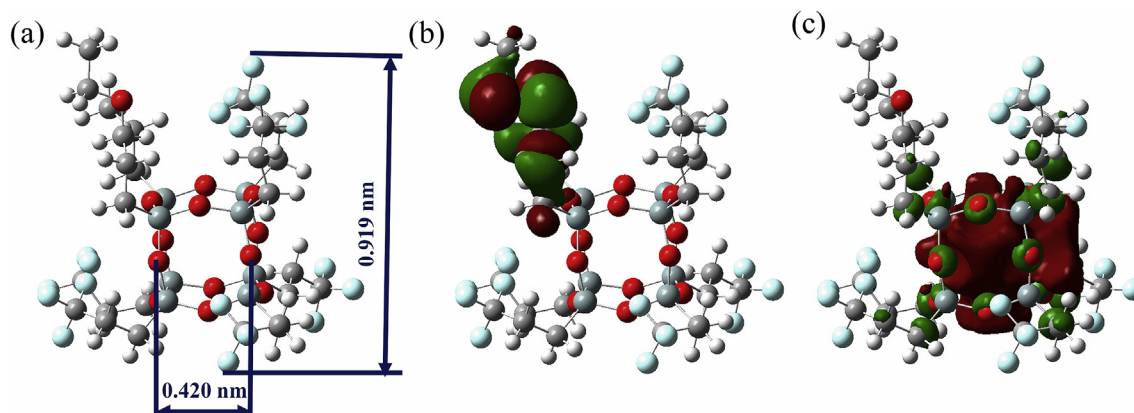


Fig. 2. Optimized structures (a) and HOMO (b) and LUMO (c) profiles of POSSs on the basis of DFT calculations at the B3LYP/6-31G(d) level.

3.3. Thermal property

The thermal properties of the copolymers were investigated using TGA and DSC, and the key parameters were summarized in Fig. 3 and Table 2. All copolymers exhibited good thermal stability with the onset decomposition temperatures (T_{d5} , measured at a 5% weight loss) from 321 to 384 °C. It is ascribed that the incorporation of the POSSs group at the side chain of fluorene maintains the high thermal stability of polyfluorenes [36]. However, the thermal stability of the copolymer wasn't further improved with the increase in the feed ratio of the POSSs, which may be attributed to the poor degree of polymerization of the polymers.

3.4. Photophysical properties

The normalized UV–vis absorption and PL spectra of the copolymers in dilute solution are shown in Fig. 4a. The absorption peaks of all copolymers are around 370 nm, which is mainly attributed to the $\pi-\pi^*$ transition in polyfluorene skeleton. With the increase of the POSSs group, the absorption peaks are slightly blue-shifted gradually from PFSDF10-POSS1 at 375 nm to PFSDF10-POSS20 at 360 nm (Table 2). This may be because the distortion of molecular chain and effective conjugate chain length of the polyfluorene is reduced by the large cage structure of the POSSs monomer, which causes the decreasing electron delocalization in polyfluorene conjugated system and the increased energy required for molecular transitions. It can be seen from the fluorescence emission spectra that all copolymers exhibit typical emission peaks of polyfluorene at 414 nm and 435 nm, respectively, which indicates the fact that the electronic structure of polyfluorene is not affected by the incorporation of POSSs group at the side chain of fluorene. The fine vibrational structures at near 435 nm can also indicate that all copolymers are similar to the rigid structure of polyfluorene. At the same time, the emission peaks do not change significantly in dilute solution with the increase of POSSs contents, which indicates the fact that the emission behavior of copolymers is not affected by the introduction of POSSs. The absorption and emission bands of DBT are not observable in the spectra owing to its comparatively low content in the copolymers.

In film state, the copolymers exhibit UV–vis absorption bands at around 375 nm owing to the $\pi-\pi^*$ transitions of the polyfluorene backbones (Fig. 4b and Table 2). The difference from that in solution is the maximum absorption band of the copolymer in film showed no obvious blue shift with the increase of POSSs content. In PL spectra, the emission peaks of polyfluorene are located at 421 nm and 449 nm and the

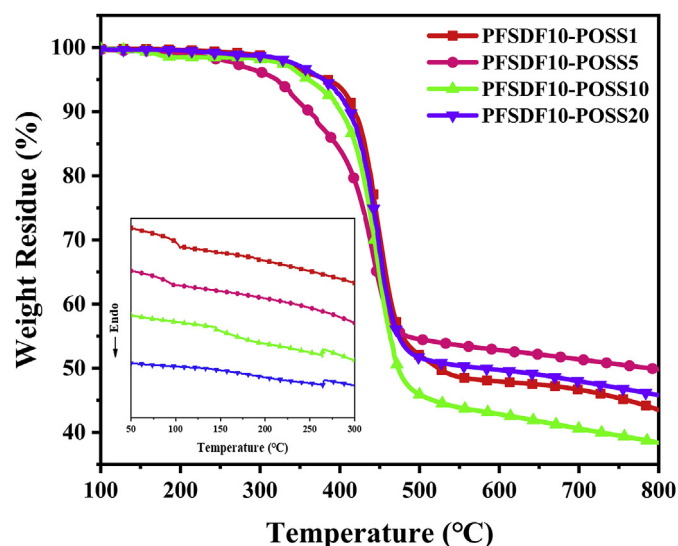


Fig. 3. TGA and DSC (insert) curves of the copolymers in nitrogen atmosphere with a heating rate of 10 °C/min and 5 °C/min, respectively.

emission peak of orange-red light group DBT is located at 624 nm, indicating that the effective Förster energy transfer occurs from the polyfluorene fragment to the DBT group, inducing the emission of orange-red light. PFSDF10-POSS1 and PFSDF10-POSS5 show no significant emission peak at 620 nm, which is attributed to the low reacted contents of DBT by one-pot Suzuki polycondensation. Moreover, the emission peaks of copolymers exhibit a slight red shift in the PL spectra compared to that in dilute solution, which may be attributed to the inhibition effect of SDF on aggregation of polymers was destroyed by the large cage structure of POSSs.

At the same time, the molecule steric hindrance is increased because the POSSs group as a substituent on the fluorene can also play a “dilution” role, avoiding the generation of excimer and ensuring the stability of spectra in different states.

As shown in Table 2, the fluorescence quantum yields of PFSDF10-POSSx copolymers in solution were 70%–80%, indicating that the electronic structure of polyfluorene system was not affected by the introduction of the POSSs group. There was no energy loss due to the cross-linking effect of SDF and POSSs structures, and the high quantum efficiency of polyfluorene materials was maintained. In addition, the lifetime properties of the copolymers in CDCl₃ solution and the detailed descriptions are displayed in Figure S9 in supplementary information.

3.5. Electrochemical properties

As shown in Fig. 5 and Table 3, the electrochemical properties of the PFSDF10-POSSx were investigated by cyclic voltammetry (CV). The oxidation potentials (E_{ox}) varied slightly from 1.00 V to 1.30 V. The HOMO levels of PFSDF10-POSSx were calculated according to the empirical formulas $E_{HOMO} = -[4.8 + (E_c^{ox} - E_f^{ox})](eV)$ [37]. The LUMO levels were deduced from the HOMO levels and the optical band gaps (E_g) determined from the onset value of the absorption spectrum in film in the long-wavelength direction $E_g = 1240/\lambda_{edge}$. The HOMO and LUMO levels of the copolymers are at about -5.70 eV and -2.50 eV, respectively, which indicate that the hole and electron injection in device are much easy through introducing the POSSs group.

3.6. Film morphology

The morphology of the spin-coated films of copolymers is a critical factor for the PLED fabrication, which was measured by atomic force microscopy (AFM) at a tapping mode and showed in Fig. 6. All the films show a flat and smooth surface without any pinhole defects. The root-mean-square (RMS) roughness values of copolymers are 0.79, 0.86, 0.52, and 0.61 nm, respectively, corresponding to the variation of content for copolymers from 1 mol% to 20 mol%. The results imply that amorphous films with good quality can be easily prepared by the synergistic influence of the introduced POSSs group and SDF branch center, which is favorable for PLEDs fabrication.

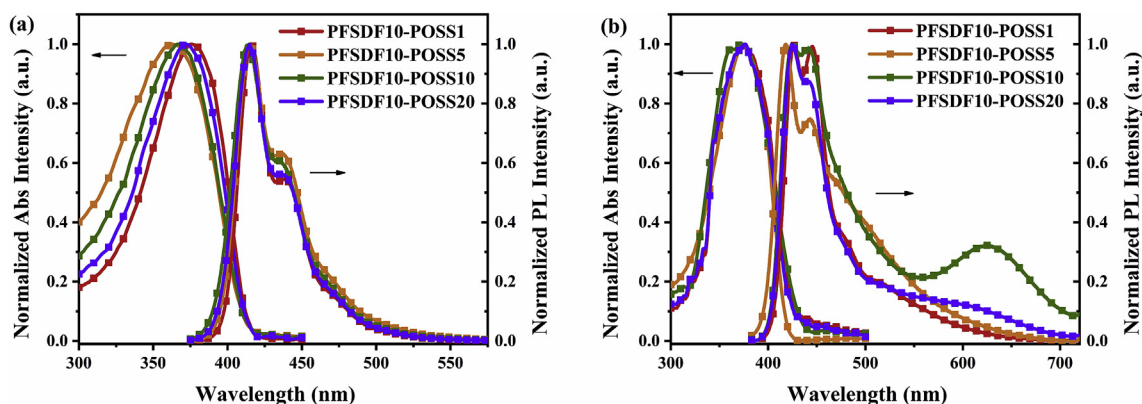
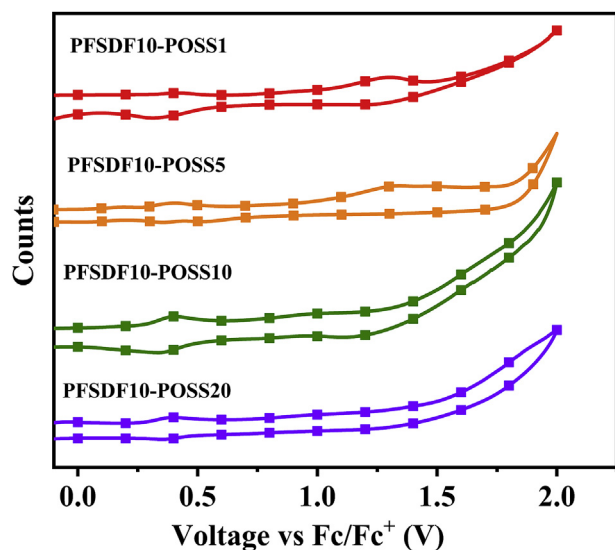
3.7. Hydrophobic properties

In previous studies, we found that PEDOT: PSS could be dissolved and then defects were formed at PEDOT: PSS/EML interface when the hyperbranched polymers emitting layer was spin-coated on the water-soluble PEDOT: PSS layer. The defects generated on PEDOT: PSS layer are easily broken down with increasing current density, which affects the device efficiency, brightness and stability of the hyperbranched PLEDs. Therefore, it is urgent to improve the hydrophobicity of the hyperbranched polymer materials, which were characterized by the water contact angles test and the results were shown in Fig. 7. The water contact angle of PFSDF10-POSS1 was 95°, while the maximum water contact angle of PFSDF10-POSS20 was 114.5°. Obviously, the water contact angle was linearly increased with the increasing components of the POSSs groups, which demonstrated that the hydrophobicity of the

Table 2

Thermal and photophysical properties of the copolymers.

Copolymer	T_d (°C)	T_g (°C)	Dilute solution		Solid film		PLQY	
			λ_{abs} (nm)	λ_{PL} (nm)	λ_{abs} (nm)	λ_{PL} (nm)	Solution (%)	Film (%)
POSS1	384	105	375	414, 435	375	421, 445	75.77	7.42
POSS5	321	104	370	414, 435	375	418, 443	76.95	5.11
POSS10	361	144	366	414, 434	370	421, 442, 625	71.37	5.80
POSS20	380	145	360	414, 434	375	421, 443, 624	70.20	13.53

**Fig. 4.** UV-vis absorption and PL spectra of copolymers: (a) in CHCl_3 solution (10^{-5} M) and (b) in solid film.**Fig. 5.** The cyclic voltammogram curves of the copolymer films.**Table 3**

Electrochemical properties of the copolymers.

Copolymers	λ_{abs} (onset) (nm)	E_g (eV)	HOMO (eV)	LUMO (eV)
PFSDf10-POSS1	425	2.92	-5.70	-2.79
PFSDf10-POSS5	423	2.93	-5.74	-2.81
PFSDf10-POSS10	422	2.94	-5.43	-2.50
PFSDf10-POSS20	420	2.95	-5.43	-2.48

hyperbranched polymer was improved effectively. This provided the basis of the enhancement of the waterproof and oxygen barrier ability of the device in the next work by the incorporation of trifluoropropyl on the peripheral groups of the POSSs group.

3.8. Electroluminescent properties

In order to reveal the EL performance of synthesized copolymers, the devices were fabricated with the configuration ITO/PEDOT: PSS (40 nm)/copolymer (50 nm)/TPBi (35 nm)/LiF (1 nm)/Al (150 nm). The structure and relative-energy-level diagram of all devices were shown in Fig. 8a and (b), respectively. ITO and Al (150 nm) are served as the anode and cathode, respectively, PEDOT: PSS (40 nm) layer is used as the hole injection and transporting layer; PFSDf10-POSSx (50 nm) layer is used as the light-emitting layer; TPBi (35 nm) and LiF (1 nm) are used as the electron-transfer and electron-injection layers no other inorganic dopants, respectively [38–48]. As shown in Fig. 7b, the HOMO and LUMO levels of the copolymers are well matched to that of TPBi and PEDOT: PSS, which effectively facilitate the injection of electron and hole carriers into light-emitting layer in fabricated PLEDs.

The electroluminescence spectra of copolymer materials at voltages varying from 5 to 10 V are displayed in Fig. 9. All copolymer-based devices exhibit much broader EL spectra than their PL spectra, covering most of the visible light region. This contributes to the almost sunlight-style white light emission with the CIE coordinates located at (0.33, 0.33). The CRI of all devices is higher than 70 and the PFSDf10-POSS5 reaches the maximum CRI value of 96 at 8 V.

4. Conclusions

In this work, a series of white polymer light-emitting materials with 9,9-dioctylfluorene, fluorine-containing polyhedral oligomeric silsesquioxanes (POSSs) modified 9,9-dioctylfluorene and 4,7-bis(2-bromo-5-thienyl)-2,1,3-benzothiadiazole (DBrDBT) as the branches, the three-dimensional structured spiro [3,3]heptane-2,6-dispirofluorene (SDF, 10 mol %) as the core were obtained through Suzuki polycondensation. It was found that the interactions between chains were effectively suppressed by the introduction of POSSs group in their PL spectra, leading to no apparent bathochromic shifts in solid films with respect to those in dilute solution. Besides, because of the large amount of fluorine element introduced in the R group of POSSs, the hydrophobicity of all materials has been dramatically improved, which enhanced the waterproof and oxygen insulation abilities of the hyperbranched polymer

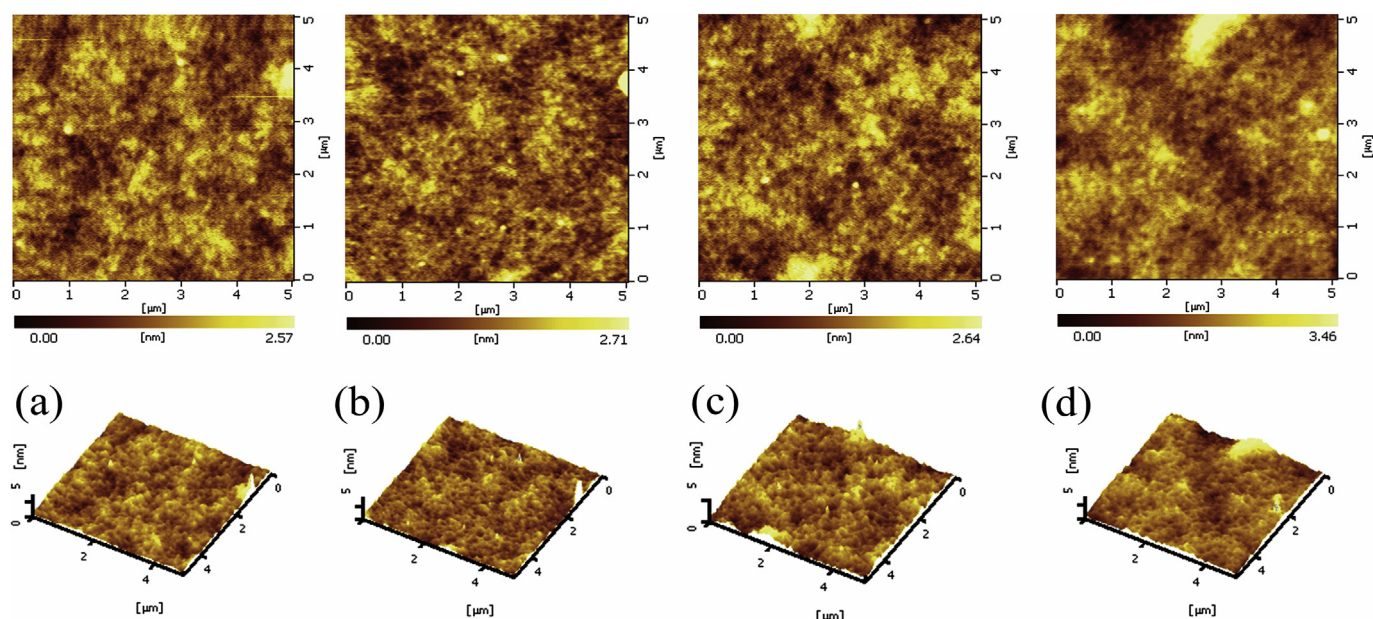


Fig. 6. AFM images ($5 \times 5 \mu\text{m}$) of the copolymer films: (a) PFSDf10-POSS1, (b) PFSDf10-POSS5, (c) PFSDf10-POSS10, (d) PFSDf10-POSS20.

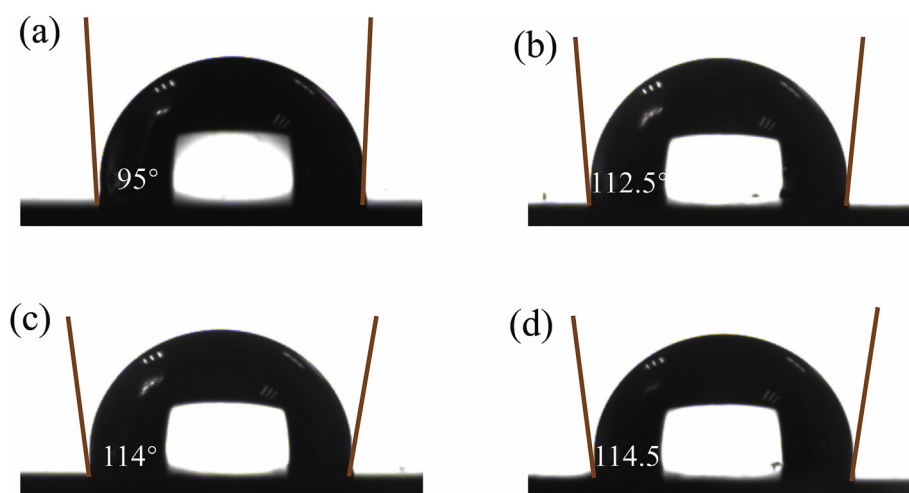


Fig. 7. Water contact angles of copolymer films: (a) PFSDf10-POSS1, (b) PFSDf10-POSS5, (c) PFSDf10-POSS10, (d) PFSDf10-POSS20.

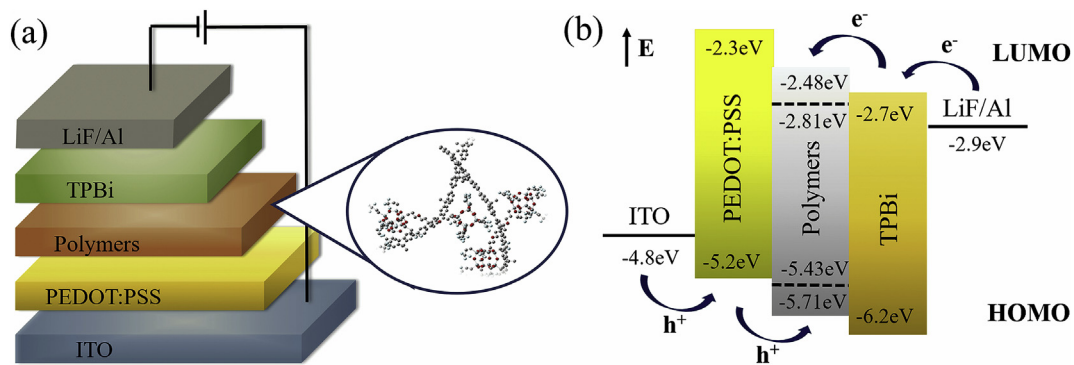


Fig. 8. Device structure (a) and energy-level (b) diagrams of OLEDs.

light-emitting devices. The optimized device with polymer light-emitting layer achieve good EL performance with CIE coordinates at (0.32, 0.33) and maximum CRI of 96. The results indicate that the

fluorene-containing POSSs modified hyperbranched white polymer light-emitting materials could be the promising candidates in WPLEDs.

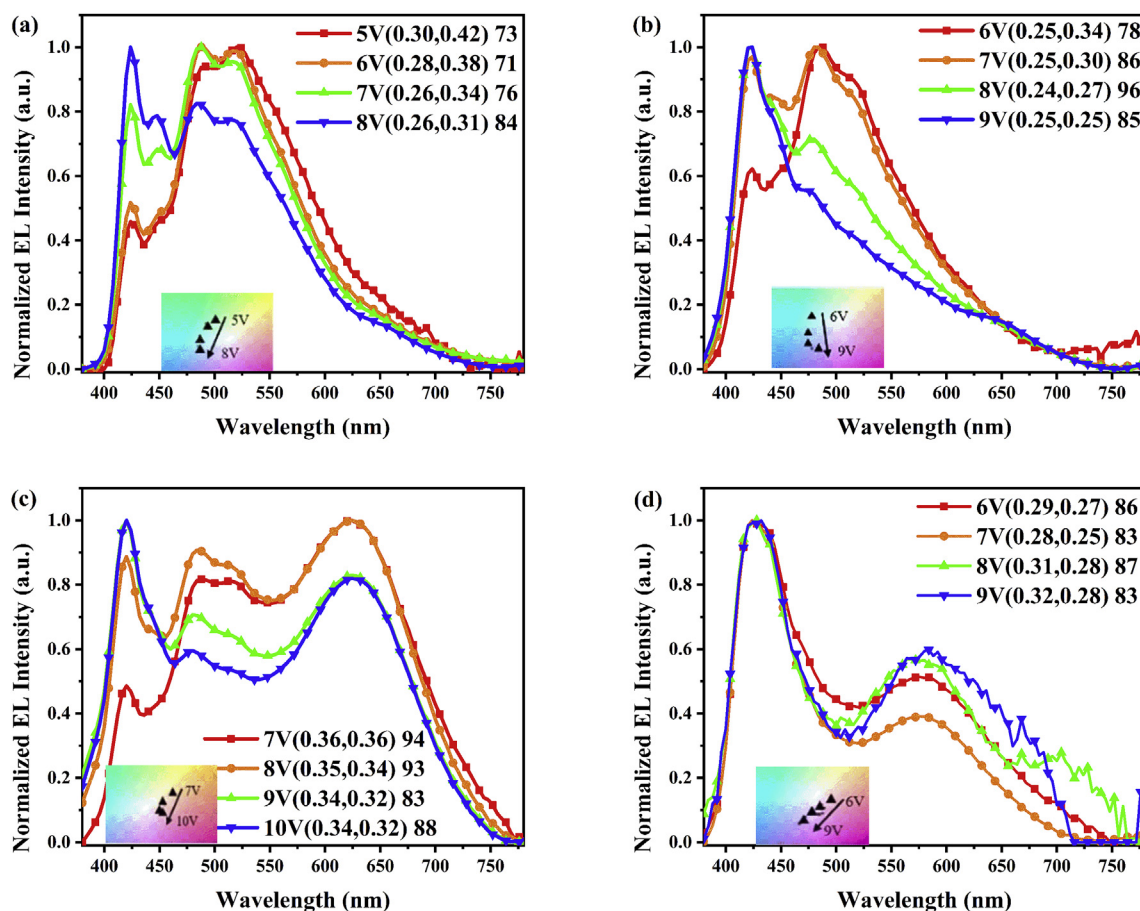


Fig. 9. EL spectra of the copolymer devices and the corresponding CIE coordinates and CRI at voltages varying from 5 V to 10 V: (a) PFSDF10-POSS1, (b) PFSDF10-POSS5, (c) PFSDF10-POSS10, (d) PFSDF10-POSS20.

CRediT authorship contribution statement

Mixue Wang: Preparation of experimental products. **Xiaozhen Wei:** Fabrication of WPLED devices. **Weixuan Zhang:** Performance test. **Haocheng Zhao:** Performance test. **Yuling Wu:** Designed molecular structure, provided financial support. **Yanqin Miao:** Designed of device structure. **Hua Wang:** Analysis experiment, provided financial support. **Bingshe Xu:** Provided the test platform.

Declaration of competing interest

The authors declare that they have no known competing financial interests or personal relationships that could have appeared to influence the work reported in this paper.

Acknowledgements

The authors are grateful to the “the National Natural Science Foundation of China (61705158, 61775155, 61705156); Key R&D program of Shanxi Province (International Cooperation, 201903D421087); Program for the Innovative Talents of Higher Education Institutions of Shanxi; Shanxi Province Natural Science Foundation (201801D221102); and Scientific and Technological Innovation Programs of Higher Education Institutions in Shanxi (2019L0302, 201802111).

Appendix A. Supplementary data

Supplementary data to this article can be found online at <https://doi.org/10.1016/j.jssc.2021.122122>.

References

- [1] G. Gustafsson, Y. Cao, G.M. Treacy, F. Klavetter, N. Colaneri, A.J. Heeger, Flexible light-emitting diodes made from soluble conducting polymers, *Nature* 357 (1992) 477–479, <https://doi.org/10.1038/357477a0>.
- [2] B.H. Zhang, G.P. Tan, C.S. Lam, B. Yao, C.L. Ho, L.H. Liu, Z.Y. Xie, W.Y. Wong, J.Q. Ding, L.X. Wang, High-efficiency single emissive layer white organic light-emitting diodes based on solution-processed dendritic host and new orange-emitting iridium complex, *Adv. Mater.* 24 (2014) 1873–1877, <https://doi.org/10.1002/adma.201104758>.
- [3] D.M. Liu, G.Y. Dong, X. Wang, F.M. Nie, X. Li, A luminescent Eu coordination polymer with near-visible excitation for sensing and its homologues constructed from 1,4-benzenedicarboxylate and 1H-imidazo[4,5-f][1,10]-phenanthroline, *CrystEngComm* 22 (2020) 7877–7887, <https://doi.org/10.1039/d0ce01256d>.
- [4] Q. Zhao, X.Y. Dai, H. Yao, Y.M. Zhang, W.J. Qu, Q. Lin, T.B. Wei, Stimuli-responsive supramolecular hydrogel with white AIE effect for ultrasensitive detection of Fe³⁺ and as rewritable fluorescent materials, *Dyes Pigments* 184 (2020) 108875–108884, <https://doi.org/10.1016/j.dyepig.2020.108875>.
- [5] G.I. Nosova, D.A. Lypenko, R.Y. Smyslov, E.V. Zhukova, I.A. Berezin, L.S. Litvinova, E.I. Maltsev, A.V. Yakimansky, Copolyfluorenes containing carbazole or triphenylamine and diethoxyphosphoryl groups in the side chains as white-light-emitting polymers, *Polymer* 210 (2020) 122978–122991, <https://doi.org/10.1016/j.polymer.2020.122978>.
- [6] Y.L. Wu, X.F. Li, H.C. Zhao, J. Li, Y.Q. Miao, H. Wang, F.R. Zhu, B.S. Xu, Pyrene-based hyperbranched porous polymers with doped Ir(piq)₂(acac) red emitter for highly efficient white polymer light-emitting diodes, *Org. Electron.* 76 (2020) 105487–105496, <https://doi.org/10.1016/j.orgel.2019.105487>.
- [7] M.C. Gather, A. Kohnen, K. Meerholz, White organic light-emitting diodes, *Adv. Mater.* 23 (2011) 233–248, <https://doi.org/10.1002/adma.201002636>.
- [8] J. Liu, Y.X. Cheng, Z.Y. Xie, Y.H. Geng, L.X. Wang, X.B. Jing, F.S. Wang, White electroluminescence from a star-like polymer with an orange emissive core and four blue emissive arms, *Adv. Mater.* 20 (2008) 1357–1362, <https://doi.org/10.1002/adma.200701705>.
- [9] L. Ying, C.L. Ho, H.B. Wu, Y. Cao, W.Y. Wong, White polymer light-emitting devices for solid-state lighting: materials, devices, and recent progress, *Adv. Mater.* 26 (2014) 2459–2473, <https://doi.org/10.1002/adma.201304784>.

- [10] C.W. Wu, H.C. Lin, Synthesis and characterization of kinked and hyperbranched carbazole/fluorene-based copolymers, *Macromolecules* 39 (2006) 7232–7240, <https://doi.org/10.1021/ma061770j>.
- [11] L.J. Twyman, A. Ellis, P.J. Gittins, Synthesis of multiporphyrin containing hyperbranched polymers, *Macromolecules* 44 (2011) 6365–6369, <https://doi.org/10.1021/ma200863u>.
- [12] A. Rehman, S.J. Park, Facile synthesis of nitrogen-enriched microporous carbons derived from imine and benzimidazole-linked polymeric framework for efficient CO₂ adsorption, *J. CO₂ Util.* 21 (2017) 503–512, <https://doi.org/10.1016/j.jcou.2017.08.016>.
- [13] A. Rehman, S.J. Park, Microporous carbons derived from melamine and isophthalaldehyde: one-pot condensation and activation in a molten salt medium for efficient gas adsorption, *Sci. Rep.* 8. 1 (2018) 1–11, <https://doi.org/10.1038/s41598-018-24308-z>.
- [14] A. Rehman, S.J. Park, Highlighting the relative effects of surface characteristics and porosity on CO₂ capture by adsorbents templated from melamine-based polyaminals, *J. Solid State Chem.* 258 (2018) 573–581, <https://doi.org/10.1016/j.jssc.2017.11.019>.
- [15] A. Rehman, S.J. Park, Influence of nitrogen moieties on CO₂ capture by polyamine-based porous carbon, *Macromol. Res.* 25 10 (2017) 1035–1042, <https://doi.org/10.1007/s13233-017-5138-1>.
- [16] S.H. Phillips, T.S. Haddad, S.J. Tomczak, Developments in nanoscience polyhedral oligomersilsesquioxane (poss)-polymers, *Curr. Opin. Solid State Mater. Sci.* 8 (2014) 21–29, <https://doi.org/10.1016/j.cossms.2004.03.002>.
- [17] R.H. Baney, M. Itoh, A. Sakakibara, T. Suzuki, Silesquioxanes, *Chem. Rev.* 95 (1995) 1409–1430, <https://doi.org/10.1021/cr00037a012>.
- [18] F. Carniato, C. Bisio, E. Boccaleri, M. Guidotti, E. Gavrilova, L. Marchese, Titanosilsesquioxane anchored on mesoporous silicas: a novel approach for the preparation of heterogeneous catalysts for selective oxidations, *Chemistry-A European Journal* 14 (2008) 8098–8102, <https://doi.org/10.1002/chem.200801241>.
- [19] P.P. Pescarmona, J.C. Waal van der, I.E. Maxwell, T. Maschmeyer, A new, efficient route to titanium-silsesquioxane epoxidation catalysts developed by using high-speed experimentation techniques, *Angew. Chem. Int. Ed.* 40 (2001) 40–43, [https://doi.org/10.1002/1521-3757\(20010216\)113:4<762::AID-ANGE7620>3.0.CO;2-8](https://doi.org/10.1002/1521-3757(20010216)113:4<762::AID-ANGE7620>3.0.CO;2-8).
- [20] A. Bukowczan, E. Hebda, M. Czajkowski, K. Pielichowski, The synthesis and properties of liquid crystalline polyurethanes, chemically modified by polyhedral oligomersilsesquioxanes, *Molecular* 24 (2019) 4013–4030, <https://doi.org/10.3390/molecules24224013>.
- [21] F. Zou, H.X. Ling, L. Zhou, F.F. Wang, Y. Li, Construction and photoluminescence properties of octaimidazolium-based polyhedral oligomeric silsesquioxanes hybrids through the ‘bridge’ of ionic liquids: chemical sensing for Cu²⁺, *Dyes Pigments* 184 (2021) 108840–108847, <https://doi.org/10.1016/j.dyepig.2020.108840>.
- [22] K. Zeng, S.X. Zheng, Nanostructures and surface dewettability of epoxy thermosets containing hepta(3,3,3-trifluoropropyl) polyhedral oligomeric silsesquioxane-capped poly(ethyleneoxide), *J. Phys. Chem. B* 111 (2007) 13919–13928, <https://doi.org/10.1021/jp075891c>.
- [23] B.R. Zeng, C.J. Yang, Y.T. Xu, W.A. Luo, L.Z. Dai, Polymerization process and performances of polymer containing polyhedral oligomeric silsesquioxanes, *Polym. Mater. Sci. Eng.* 28 (2012) 185–189, <https://doi.org/10.16865/j.cnki.1000-7555.2012.06.045>.
- [24] L. Wang, K. Zeng, S.X. Zheng, Hepta(3,3,3-trifluoropropyl) polyhedral oligomeric silsesquioxane-capped Poly(N-isopropylacrylamide) telechelics: synthesis and Behavior of Physical Hydrogels, *ACS Appl. Mater. Interfaces* 3 (2011) 898–909, <https://doi.org/10.1021/am101258k>.
- [25] K. Zeng, L. Wang, S.X. Zheng, Rapid deswelling and reswelling response of poly(N-isopropylacrylamide) hydrogels via formation of interpenetrating polymer networks with polyhedral oligomeric silsesquioxane-capped poly(ethylene oxide) amphiphilic telechelics, *J. Phys. Chem. B* 113 (2009) 11831–11840, <https://doi.org/10.1021/jp9043623>.
- [26] K. Zeng, Y.H. Liu, S.X. Zheng, Poly(ethylene imine) hybrids containing polyhedral oligomeric silsesquioxanes: preparation, structure and properties, *Eur. Polym. J.* 44 (2008) 3946–3956, <https://doi.org/10.1016/j.eurpolymj.2008.07.049>.
- [27] K. Zeng, L. Wang, S.X. Zheng, X.F. Qian, Self-assembly behavior of hepta(3,3,3-trifluoropropyl) polyhedral oligomeric silsesquioxane-capped poly(3-caprolactone) in epoxy resin: nanostructures and surface properties, *Polymer* 50 (2009) 685–695, <https://doi.org/10.1016/j.polymer.2008.11.024>.
- [28] W.L. Yu, J. Pei, W. Huang, A.J. Heeger, Spiro-functionalized polyfluorene derivatives as blue light-emitting materials, *Adv. Mater.* 12 (2000) 828–832, [https://doi.org/10.1002/\(SICI\)1521-4095\(200006\)12:11<828::AID-ADMA828>3.0.CO;2-H](https://doi.org/10.1002/(SICI)1521-4095(200006)12:11<828::AID-ADMA828>3.0.CO;2-H).
- [29] C. He, L.W. Li, W.D. He, W.X. Jiang, C. Wu, Click long seesaw-type A~B~A chains together into huge defect-free hyperbranched polymer chains with uniform subchains, *Macromolecules* 44 (2011) 6233–6236, <https://doi.org/10.1021/ma2013783>.
- [30] D. Konkolewicz, C.K. Poon, A. Gray-Weale, S. Perrier, Hyperbranched alternating block copolymers using thiol-yne chemistry: materials with tuneable properties, *Chem. Commun.* 47 (2011) 239–241, <https://doi.org/10.1039/C0CC02429E>.
- [31] L.R. Tsai, Y. Chen, Hyperbranched poly(fluorenevinylenes) obtained from self-polymerization of 2,4,7-Tris(bromomethyl)-9,9-dihexylfluorene, *Macromolecules* 41 (2008) 5098–5106, <https://doi.org/10.1021/ma800545z>.
- [32] W. Shin, M.Y. Jo, D.S. You, Y.S. Jeong, D.Y. Yoon, J.W. Kang, J.H. Cho, G.D. Lee, S.S. Hong, J.H. Kim, Improvement of efficiency of polymer solar cell by incorporation of the planar shaped monomer in low band gap polymer, *Synth. Met.* 162 (2012) 768–774, <https://doi.org/10.1016/j.synthmet.2012.02.004>.
- [33] Z. Wang, P. Lu, S. Xue, C. Gu, Y. Lv, Q. Zhu, H. Wang, Y. Ma, A solution-processable deep red molecular emitter for non-doped organic red-light-emitting diodes, *Dyes Pigments* 91 (2011) 356–363, <https://doi.org/10.1016/j.dyepig.2011.03.034>.
- [34] B. Liu, A. Najari, C. Pan, M. Leclerc, D. Xiao, Y. Zou, New low bandgap dithienylbenzothiadiazole vinylene based copolymers: synthesis and photovoltaic properties, *Macromol. Rapid Commun.* 31 (2010) 391–398, <https://doi.org/10.1002/marc.200900654>.
- [35] Y.L. Wu, J. Li, W.Q. Liang, J.L. Yang, J. Sun, H. Wang, X.G. Liu, B.S. Xu, W. Huang, Fluorene-based hyperbranched copolymers with spiro[3.3]heptane-2,6-dispirofluorene as the conjugation-uninterrupted branching point and their application in WPLEDs, *New J. Chem.* 39 (2015) 5977–5983, <https://doi.org/10.1039/C5NJ00667H>.
- [36] J.H. Lee, H.J. Cho, B.J. Jung, N.S. Cho, H.K. Shim, Stabilized blue luminescent polyfluorenes: introducing polyhedral oligomeric silsesquioxane, *Macromolecules* 37 (2004) 8523–8529, <https://doi.org/10.1021/ma0497759>.
- [37] J. Yang, C.Y. Jiang, Y. Zhang, R.Q. Yang, W. Yang, Q. Hou, Y. Cao, High-efficiency saturated red emitting polymers derived from fluorene and naphthoselenadiazole, *Macromolecules* 37 (2004) 1211–1218, <https://doi.org/10.1021/ma035743u>.
- [38] Y.Q. Miao, P. Tao, K.X. Wang, H.X. Li, B. Zhao, L. Gao, L. Wang, B.S. Xu, Q. Zhao, Highly efficient red and white organic light-emitting diodes with external quantum efficiency beyond 20% by employing pyridylimidazole-based metallophosphors, *ACS Appl. Mater. Interfaces* 9 (2017) 37873–37882, <https://doi.org/10.1021/acsami.7b10300>.
- [39] G. Nazir, H. Kim, J.H. Kim, K.S. Kim, D.H. Shin, M.F. Khan, D.S. Lee, J.Y. Hwang, C.Y. Hwang, J.H. Suh, J.H. Eom, S.Y. Jung, Ultimate limit in size and performance of WSe₂ vertical diodes, *Nat. Commun.* 9 (2018) 1–9, <https://doi.org/10.1038/s41467-018-07820-8>.
- [40] X. Liang, F. Zhang, Z.P. Yan, Z.G. Wu, Y.X. Zheng, G. Cheng, Y. Wang, J.L. Zuo, Y. Pan, C.M. Che, Fast synthesis of iridium(III) complexes incorporating a bis(diphenylphorothioyl)amide ligand for efficient pure green OLEDs, *ACS Appl. Mater. Interfaces* 11 (2019) 7184–7191, <https://doi.org/10.1021/acsami.8b19318>.
- [41] C. Wongsilarat, S. Namuangruk, N. Prachumrak, T. Sudyoadsuk, V. Promarak, M. Sukwattanasinitt, P. Rashatasakhorn, Solution processed blue-emitting and hole transporting materials from truxene-carbazole-pyrene triads, *Org. Electron.* 5 (2018) 352–358, <https://doi.org/10.1016/j.orgel.2018.03.035>.
- [42] G. Nazir, A. Rehman, S.J. Park, Energy-efficient tunneling field-effect transistors for low-power device applications: challenges and opportunities, *ACS Appl. Mater. Interfaces* 12 (2020) 47127–47163, <https://doi.org/10.1021/acsami.0c10213>.
- [43] D. Zhao, W. Huang, Z.N. Qin, Z.J. Wang, J.S. Yu, Emission spectral stability modification of tandem organic light-emitting diodes through controlling charge carrier migration and outcoupling efficiency at intermediate/emitting unit interface, *ACS Omega* 3 (2018) 3348–3356, <https://doi.org/10.1021/acsomega.8b00314>.
- [44] Y.Q. Miao, K.X. Wang, L. Gao, B. Zhao, H. Wang, F.R. Zhu, B.S. Xu, D.G. Ma, Precise manipulation of the carrier recombination zone: a universal novel device structure for highly efficient monochrome and white phosphorescent organic light emitting diodes with extremely small efficiency roll-off, *J. Mater. Chem. C* 6 (2018) 8122–8152, <https://doi.org/10.1039/C8TC02479K>.
- [45] G. Nazir, M.F. Khan, I. Akhtar, K. Akbar, P. Gautam, H.Y. Noh, Y.H. Seo, S.H. Chun, J.H. Eom, Enhanced photoresponse of ZnO quantum dot-decorated MoS₂ thin films, *RSC Adv.* 7 (2017) 16890–16900, <https://doi.org/10.1039/c7ra01222e>.
- [46] Y.Q. Miao, K.X. Wang, B. Zhao, L. Gao, P. Tao, X.G. Liu, Y.Y. Hao, H. Wang, B.S. Xu, F.R. Zhu, High-efficiency/CRI/color stability warm white organic light-emitting diodes by incorporating ultrathin phosphorescence layers in a blue fluorescence layer, *Nanophotonics* 7 (2018) 295–304, <https://doi.org/10.1515/nanoph-2017-0021>.
- [47] R.Z. Cui, W.Q. Liu, L. Zhou, X.S. Zhao, Y.L. Jiang, Y.J. Cui, Q. Zhu, Y.X. Zheng, H.J. Zhang, Green phosphorescent organic electroluminescent devices with 27.9% external quantum efficiency by employing a terbium complex as a co-dopant, *J. Mater. Chem. C* 7 (2019) 7953–7958, <https://doi.org/10.1039/C9TC02215E>.
- [48] G. Nazir, A. Ahmad, M.F. Khan, S. Tariq, Putting DFT to the trial: first principles pressure dependent analysis on optical properties of cubic perovskite SrZrO₃, *Comput. Condens. Matter* 4 (2015) 32–39, <https://doi.org/10.1016/j.cocom.2015.07.002>.